

Martensite Formation in Partially and Fully Austenitic Plain Carbon Steels

S.M.C. VAN BOHEMEN and J. SIETSMA

The progress of martensite formation in plain carbon steels Fe-0.46C, Fe-0.66C, and Fe-0.80C has been investigated by dilatometry. It is demonstrated that carbon enrichment of the remaining austenite due to intercritical annealing of Fe-0.46C and Fe-0.66C does not only depress the start temperature for martensite, but also slows the progress of the transformation with temperature compared to full austenitization. In contrast, such a change of kinetics is not observed when the remaining austenite of lean-Si steel Fe-0.80C is stabilized due to a partial transformation to bainite, which suggests that the stabilization is not of a chemical but of a mechanical nature. The growth of bainite and martensite is accompanied by a shape change at the microstructural scale, which leads to plastic deformation and thus strengthening of the surrounding austenite. Based on this stabilizing mechanism, the athermal transformation kinetics is rationalized by balancing the increase in driving force corresponding to a temperature decrease with the increase in strain energy required for the formation of martensite in the strengthened remaining austenite.

DOI: 10.1007/s11661-009-9796-2

© The Author(s) 2009. This article is published with open access at Springerlink.com

I. INTRODUCTION

IN steels, the transformation from austenite to martensite usually takes place due to a decreasing temperature rather than as a function of time, which is referred to as an athermal transformation.^[1–6] It is well known that the mechanism of growth is displacive, but how the phase nucleates and which material properties determine the amount of martensite formed is even today not completely understood despite all the efforts to study this transformation in various systems. Besides the fundamental interest in the nature of the transformation, a better understanding of the material properties that influence the progress of the martensitic transformation can also be important in the development of new advanced high-strength steels (*e.g.*, dual-phase steels), because the mechanical properties are, to a large degree, dictated by both the volume fraction and distribution of martensite in the microstructure.

In the present study, dilatometry measurements have been conducted on three plain carbon steels with different carbon content to determine the progress of the austenite to martensite transformation. The primary aim of this investigation is to get a better understanding of the differences in the kinetics of martensite formation in lean-Si steels with a bainitic/austenitic or ferritic/austenitic microstructure as compared to a fully

austenitic microstructure. Due to the low Si content (<0.4 wt pct) of the steels studied, it is reasonable to assume that carbide precipitation during the partial bainitic transformation is not retarded, which means that no significant carbon enrichment of the remaining austenite takes place. All the experimental fraction curves are analyzed using the Koistinen–Marburger (KM) equation^[5,6] and yield valuable information on the stabilization mechanism of the austenite in the partially transformed samples.

In the second part of this investigation, we attempt to get more insight into the role of the austenite grain boundaries in the nucleation and growth of martensite. Although it is known that the M_s temperature decreases with grain refinement,^[7–11] it is not well understood why the overall progress of martensite formation is virtually independent of the prior austenite grain size except for the early stage of transformation. The Greninger–Troiano metallographic technique^[1] has been applied to get a better understanding of the spatial evolution of martensite in an austenitic matrix.

II. EXPERIMENTAL

The chemical composition of the three plain carbon steels used in the present study (Fe-0.46C, Fe-0.66C, and Fe-0.80C) was measured with X-ray fluorescence (XRF) and is given in Table I. The cylindrical dilatometric samples were machined with a length of 10 mm and a diameter of 5 mm, and the dilatation of the samples as a function of temperature and time was measured at Delft University of Technology using a Bähr 805 A/D dilatometer (Bähr-Thermoanalyse GmbH, Hüllhorst, Germany).^[12] The temperature was controlled using a thermocouple spot welded onto the center of the sample.

S.M.C. VAN BOHEMEN, Researcher, formerly with the Department of Materials Science and Engineering, Delft University of Technology, Mekelweg 2, 2628 CD Delft, The Netherlands, is with Corus Research Development & Technology, 1970 CA IJmuiden, The Netherlands. Contact e-mail: s.m.c.vanbohemem@gmail.com
J. SIETSMA, Associate Professor, is with the Department of Materials Science and Engineering, Delft University of Technology.

Manuscript submitted July 15, 2008.

Article published online February 21, 2009

Table I. Chemical Composition of the Steels (Weight Percent) Together with the Parameters α_m , T_{KM} , and M_s Derived from Figure 1

Alloy	C	Mn	Si	Ni	Cr	Cu	P	S	α_m (K ⁻¹)	T_{KM} (°C)	M_s (°C)
Fe-0.46C	0.46	0.71	0.26	0.1	0.2	0.23	0.002	0.03	0.0168	308	315
Fe-0.66C	0.66	0.69	0.3	0.1	0.2	0.17	—	0.03	0.0146	258	264
Fe-0.80C	0.80	0.61	0.3	0.2	0.3	0.23	0.012	0.04	0.0131	219	231

Table II. Experimental Details and Results of Martensite Formation in the Remaining Austenite after Intercritical Annealing of Fe-0.46C and Fe-0.66C

Alloy	T_{ic} (°C)	t_{ic} (Min)	f^{a}	x_C^{γ} (Wt Pct)	T_{KM} (°C)	α_m (K ⁻¹)
Fe-0.46C	724	30	0.41	0.77	233	0.0135
Fe-0.46C	731	20	0.34	0.69	248	0.0142
Fe-0.46C	736	12	0.30	0.65	255	0.0145
Fe-0.66C	726	15	0.18	0.80	236	0.0134
Fe-0.66C	740	8	0.09	0.72	250	0.0140

To investigate the influence of the carbon content on the evolution of martensite formation, three different heat treatments were applied to three steel grades. In treatment 1, the three steels were fully austenitized at $T_{aus} = 900$ °C for 2 minutes and subsequently cooled to room temperature in the dilatometer. In treatment 2, measurements were performed to determine the martensitic transformation kinetics for Fe-0.46C and Fe-0.66C when quenching from an intercritical (in the $\alpha + \gamma$ region of the phase diagram) holding. To this purpose, the as-received steels with a ferritic-pearlitic microstructure were heated to various temperatures in the range of 720 °C to 740 °C (Table II), held at that temperature to form, besides ferrite, a certain fraction of austenite, and subsequently cooled to room temperature, during which the austenite transforms to martensite. In treatment 3, dilatometry experiments were performed on steel Fe-0.80C to investigate the effect of a partial pearlitic or bainitic transformation on the progress of the subsequent transformation of the remaining austenite to martensite. For this, fully austenitized samples were rapidly cooled to various temperatures in the range of 275 °C to 425 °C and held at that temperature for a specific time to partially transform the austenite to bainite (Table III). The transformation was interrupted and, during the cooling, the remaining austenite transformed to martensite. The volume fraction of bainite at the end of the bainitic holding was determined from the measured dilatation signal, normalizing to the dilatation corresponding to the full transformation to bainite for Fe-0.80C. The fraction bainite is linearly related to the dilatation accompanying the transformation.

For an unambiguous analysis of the dilatometry results, it is important to have an estimate of the thermal gradient in the axial direction of the sample, and therefore, a second thermocouple was welded approximately 4 mm from the center of the sample in some of the experiments. In order to minimize thermal gradients in the sample, which can lead to inaccuracies in the measured kinetics, helium quench gas was not used in

Table III. Partial Bainitic Transformation Experiments on Fe-0.80C; $\alpha_m = 0.0131$ K⁻¹ for All Experiments

T_b (°C)	t_b (Min)	f^{b}	T_{KM} (°C)
275	9	0.52	174
275	25	1	—
325	2	0.11	209
325	3	0.29	200
325	4	0.49	185
325	5	0.70	167
325	6	0.84	153
325	12	1	—
375	1.5	0.48	193
375	5	1	—
425	0.5	0.47	199
425	3	1	—
650*	1	0.61	215
650*	5	1	—

*Pearlite formation.

the temperature range of martensite formation. For example, in a typical experiment, to measure the martensitic transformation kinetics in the fully austenitic steels Fe-0.46C, Fe-0.66C, and Fe-0.80C, each sample was cooled to approximately 350 °C with a cooling rate in the range of 70 °C/s to 100 °C/s using He gas, followed by natural cooling to room temperature. The dilatation as a function of temperature indicated that no ferrite or bainite formation occurred during cooling with the cooling rates employed. The experimental results were highly reproducible, and also samples that were given a homogenization treatment prior to the heat treatment showed identical results as the as-received samples, which indicates that the distribution of substitutional elements such as Mn is homogeneous in the as-received material.

The final microstructures of the dilatometry samples were characterized using optical microscopy in order to confirm the presence of ferrite in the intercritically annealed steels Fe-0.46C and Fe-0.66C, and to demonstrate the existence of bainite in the partially transformed sample Fe-0.80C. Furthermore, the volume fractions were determined from the micrographs for comparison with the volume fractions evaluated from the dilatometry curves.

III. RESULTS

A. Composition Dependence of $\gamma \rightarrow \alpha'$

According to the method explained in Reference 13, the fraction of martensite as a function of temperature

was determined from dilatation curves measured during cooling of steels Fe-0.46C, Fe-0.66C, and Fe-0.80C with a fully austenitic microstructure (Figure 1). The solid lines through the data represent least-squares fits to the KM equation,^[5] which describes the volume fraction of martensite as a function of temperature as

$$f = 1 - \exp(-\alpha_m(T_{KM} - T)) \quad [1]$$

in which α_m is the rate parameter^[6] and T_{KM} the so-called theoretical martensite-start temperature, which can be somewhat lower than M_s (Figure 1) depending on the austenitizing treatment, as will be explained in detail later in this article. The values of T_{KM} and α_m extracted from the least-squares fits are given in Table I.

Comparison of the experimental fraction curves shown in Figure 1 and the values of α_m given in Table I strongly suggests that the chemical composition determines the progress of transformation not only by its effect on M_s , but also the kinetics, *i.e.*, the increase in volume fraction of martensite with decreasing temperature below M_s , is dependent on the composition. To strengthen this proposition, the composition dependence of the martensitic transformation kinetics has been systematically investigated by the present authors^[14] on the basis of complementary experimental data reported in the literature on the progress of martensite formation in other Fe alloys.^[15,16] Based on the fits of all experimental data to Eq. [1], it was proposed that the composition dependence of the rate parameter α_m can be described by a simple linear equation, similar to the well-known Andrews' empirical relationship between M_s and composition,^[17] as

$$\alpha_m(\text{K}^{-1}) = 0.0224 - 0.0107x_C - 0.0007x_{Mn} - 0.00005x_{Ni} - 0.00012x_{Cr} - 0.0001x_{Mo} \quad [2]$$

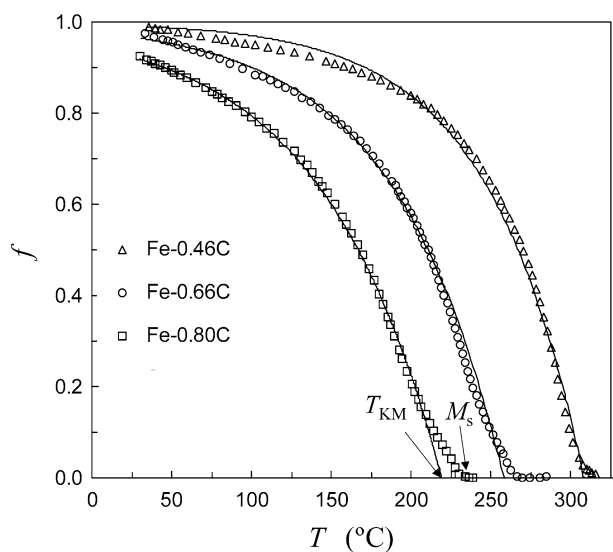


Fig. 1—Experimental and calculated curves of the martensite fraction f as a function of temperature T for steels Fe-0.46C, Fe-0.66C, and Fe-0.80C.

with the concentration x in weight percent. Also, an empirical equation for T_{KM} was determined, which yields

$$T_{KM}(\text{°C}) = 462 - 273x_C - 26x_{Mn} - 16x_{Ni} - 13x_{Cr} - 30x_{Mo} \quad [3]$$

The coefficients in this equation are in fair agreement with those in the empirical equations of M_s , as reported in References 18 and 19. Based on the evidence of Figure 1, and more generally on the composition dependence of α_m , it would be expected that in the case of chemical stabilization (carbon enrichment) of the austenite during intercritical annealing, as for example, in the processing of dual phase steels, the martensitic transformation in the remaining austenite does, as a consequence of the higher carbon content, not only start at lower temperature but also evolve at a lower rate compared to the transformation in fully austenitized steel. In order to verify this, the martensitic transformation in intercritically annealed samples of Fe-0.46C and Fe-0.66C was investigated.

B. Effect of Intercritical Annealing on $\gamma_R \rightarrow \alpha'$

The intercritical annealing temperature T_{ic} of Fe-0.46C and Fe-0.66C was varied to obtain different volume fractions of remaining austenite ($1 - f^{a_a}$) with different carbon contents (Table II). The carbon content of the intercritical austenite is calculated by

$$x_C^{\gamma} = \frac{x_0 - f^{a_a} x_C^{\alpha}}{1 - f^{a_a}} \quad [4]$$

with f^{a_a} the volume fraction of allotriomorphic ferrite. The equilibrium concentration of carbon in ferrite x_C^{α} is in the range of 0.015 to 0.02 wt pct for the chosen temperatures T_{ic} . Figure 2(a) shows the ferrite-martensite microstructure of the Fe-0.46C sample that was annealed at $T_{ic} = 736$ °C for 12 minutes and subsequently cooled to room temperature. The volume fraction of ferrite in the microstructure is in fair agreement with the fraction $f^{a_a} = 0.30$ given in Table II. The progress of martensite formation in the remaining austenite was determined from the dilatometry curves analogous to the method described in Reference 13. Figure 3 shows the martensite fraction curves for three Fe-0.46C samples that were, respectively, fully austenitized, annealed at $T_{ic} = 736$ °C and $T_{ic} = 724$ °C. The solid lines represent the best fits according to

$$f = f^{a_a} + (1 - f^{a_a})(1 - \exp(-\alpha_m(T_{KM} - T))) \quad [5]$$

in which T_{KM} and α_m are, respectively, the start temperature and rate parameter for martensite formation in the remaining austenite. For the Fe-0.46C sample annealed at $T_{ic} = 736$ °C, which has a volume fraction of allotriomorphic ferrite $f^{a_a} = 0.30$ and $x_C^{\gamma} = 0.65$ wt pct, $T_{KM} = 255$ °C, and $\alpha_m = 0.0145$ K⁻¹. These values of T_{KM} and α_m are in close agreement with the values determined for fully austenitic samples Fe-0.66C (Table I). Furthermore, it is noted that the extracted fit

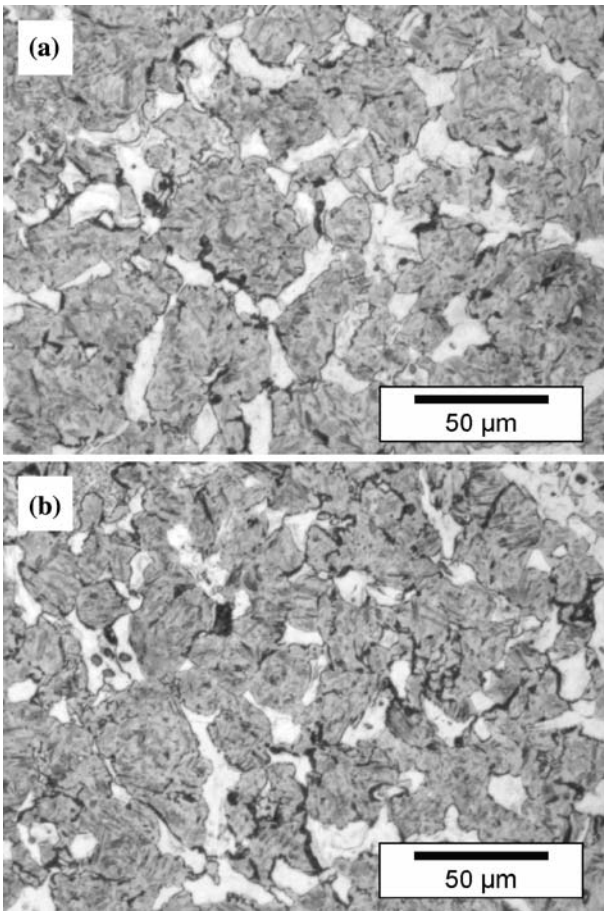


Fig. 2—Microstructures of (a) Fe-0.46C intercritically annealed at $T_{ic} = 736$ °C and (b) Fe-0.66C annealed at $T_{ic} = 726$ °C showing ferrite and martensite.

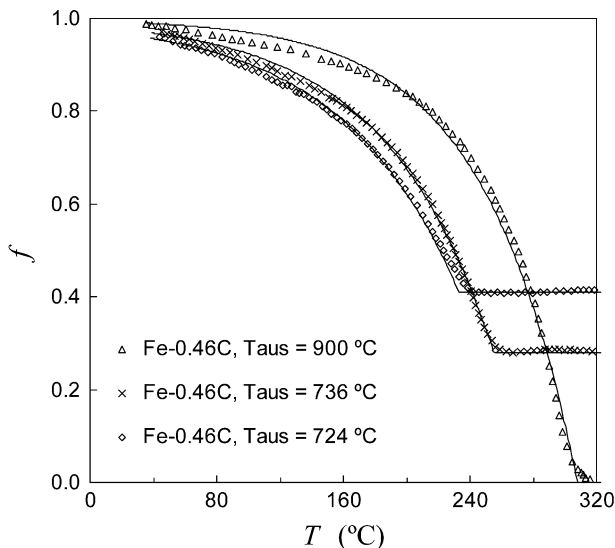


Fig. 3—Fraction f of martensite as a function of temperature T in Fe-0.46C samples intercritically annealed at 736 °C and 724 °C. The solid lines represent the best fits with the KM equation from which the start temperature and the rate parameter are extracted. As a reference, the progress of the transformation in a fully austenitic sample from Figure 1 is also shown.

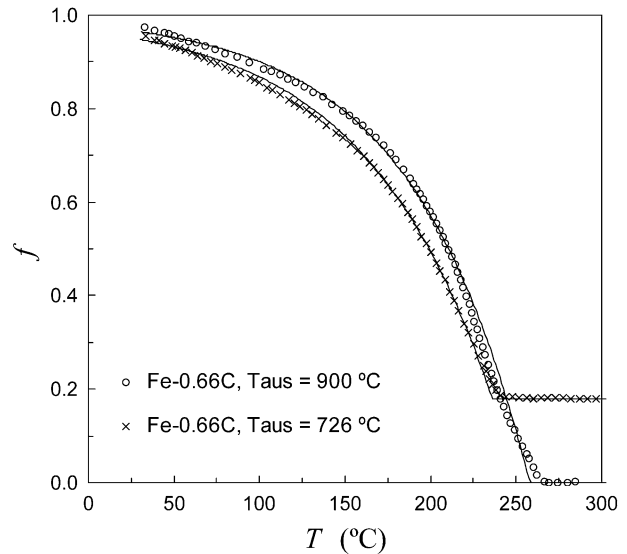


Fig. 4—Progress of martensite formation (fraction f) as a function of temperature T in Fe-0.66C intercritically annealed at 726 °C compared to the kinetics in a fully austenitic sample.

parameters $T_{KM} = 235$ °C and $\alpha_m = 0.0136$ K $^{-1}$ ($f^{\alpha_a} = 0.41$ and $x_C^\gamma = 0.77$ wt pct) for the sample annealed at $T_{ic} = 724$ °C approach the kinetic parameters of Fe-0.80C (Table I), indicating that the remaining austenite has a nearly eutectoid composition. For Fe-0.66C, similar results were obtained, as seen in Figure 4, which shows the fraction curves for both a fully austenitized sample and a sample annealed at $T_{ic} = 726$ °C. The ferrite-martensite microstructure of the Fe-0.66C sample annealed at $T_{ic} = 726$ °C is shown in Figure 2(b). The values of T_{KM} and α_m derived from the best fits for Fe-0.66C are also listed in Table II.

Analysis of the values of T_{KM} and α_m derived for all intercritical annealed samples of Fe-0.46C and Fe-0.66C given in Table II shows a clear correlation, which confirms that α_m is changed due to chemical stabilization of austenite. All the parameters α_m and T_{KM} from Table I and Table II are plotted in Figure 5 (solid squares) to demonstrate this correlation. The linear trend in the solid squares is consistent with Eqs. [2] and [3]. The error bars in Figure 5 give a measure of the inaccuracy in the evaluated fit parameters α_m and T_{KM} and are determined by the calculation of fraction curves that deviate from the best fits but are still acceptable. The inaccuracy appears to be somewhat larger when the volume fraction of remaining austenite is smaller.

C. Effect of a Partial Bainitic Transformation on $\gamma_R \rightarrow \alpha'$

In this section, the effect of a partial bainitic transformation on the subsequent transformation of the remaining austenite to martensite is discussed. A recent study by Jacques *et al.* showed that the bainitic transformation of a 0.38 wt pct Si steel goes nearly to completion.^[20] Based on Mössbauer spectroscopy, they found that the final microstructure contained less than 2 vol pct retained austenite, probably present in the

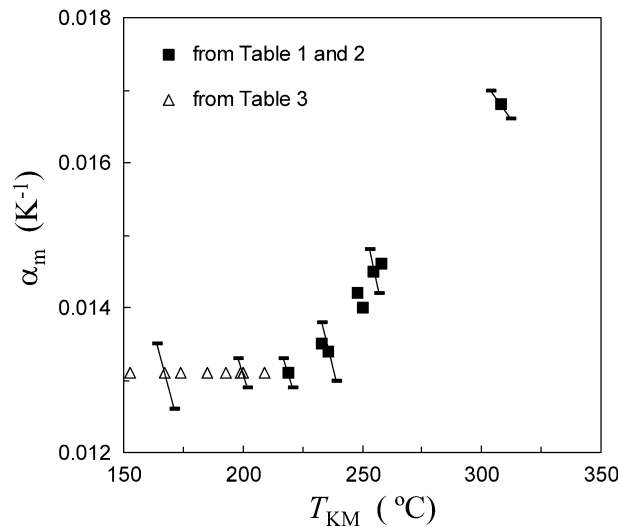


Fig. 5—Correlation between the KM parameters α_m and T_{KM} (Eq. [1]) for a fully austenitic or a ferritic/austenitic microstructure (Tables I and II) is different from the relationship between α_m and T_{KM} for a bainitic/austenitic microstructure (Table III).

form of thin austenite films between the bainitic platelets and, therefore, not visible in SEM micrographs. Based on the result from Reference 20, that carbon enrichment of the remaining austenite in a steel with 0.38 wt pct Si is negligibly small, steel Fe-0.80C with approximately 0.3 wt pct Si was chosen in the present study to examine the effect of a partially bainitic transformation, during which x_C^{γ} can be assumed constant, on the subsequent decomposition of the remaining austenite to martensite. The evolution of martensite in partially bainitic samples is compared to the results obtained for intercritically annealed samples, which can be well explained by chemical stabilization of the remaining austenite, as demonstrated earlier.

Samples of Fe-0.80C were austenitized at 800 °C for 1 minute and subsequently held at various temperatures to investigate the stabilization effect of the formation of bainite on the remaining austenite. The isothermal transformation was interrupted at various stages, and during cooling, the start and progress of martensite formation in the remaining austenite was measured by dilatometry. The details of the partial transformation experiments are listed in Table III. As an example, three fraction curves are shown in Figure 6 for samples that were partially transformed to bainite at 325 °C for different times. The solid lines through the data are the best fits calculated with Eq. [5], and it is found that all experimental fraction curves can be well described using $\alpha_m = 0.0131 \text{ K}^{-1}$, which is equal to the rate parameter for martensite formation in a fully Fe-0.80C austenitic sample austenitized at 800 °C for 1 minute. For comparison, the fraction curve corresponding to this fully austenitic sample is also shown in Figure 6. The values of T_{KM} derived from the best fits are given in Table III. Figure 7 shows the micrographs of samples that were isothermally held at 325 °C for 2, 4, and 6 minutes. These microstructures demonstrate the evolution of bainite formation, and the corresponding volume

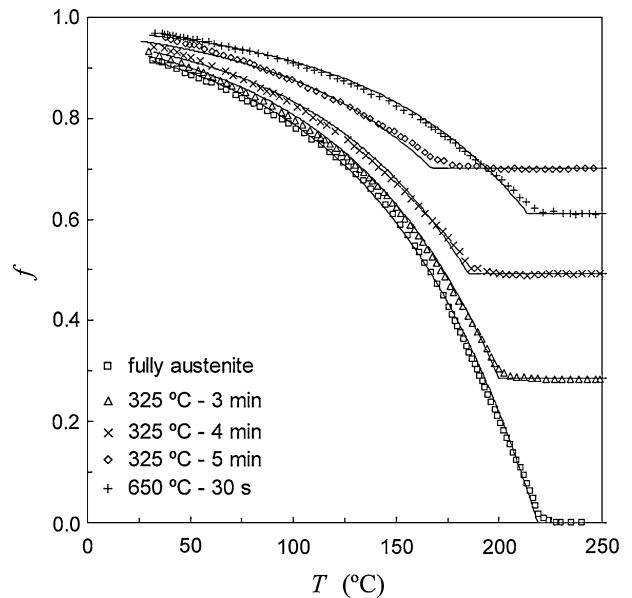


Fig. 6—Fraction of martensite f as a function of temperature T in Fe-0.80C samples partially transformed to bainite at 325 °C for 3, 4, and 5 min. The solid lines represent the fits with the KM equation from which the start-temperature T_{KM} is extracted; $\alpha_m = 0.0131 \text{ K}^{-1}$ for all curves. For comparison, the transformations in a fully austenitic sample (open squares) and a partially pearlitic sample (+) are also shown.

fractions given in the caption of Figure 7 roughly agree with the values listed in Table III.

The values of T_{KM} are plotted against the volume fraction of bainite in Figure 8. For the different transformation times at $T_b = 325 \text{ °C}$, it is seen that T_{KM} decreases approximately linearly with the fraction transformed. Also, the dependence of T_{KM} on the bainite transformation temperature was investigated. At the other temperatures, a fraction of bainite of about 0.5 was formed, and Figure 8 shows that the stabilization effect becomes stronger at lower temperatures.

Figure 6 also shows the evolution of martensite formation in a sample that was partially transformed (61 vol pct) to pearlite at 650 °C. Also, the kinetics of martensite formation in this partially pearlitic sample can be well described using a rate parameter $\alpha_m = 0.0131 \text{ K}^{-1}$, and a smaller depression of T_{KM} is observed as compared to the partially bainitic samples (also Figure 8).

The observation in Figure 8 that T_{KM} decreases with increasing fraction of bainite indicates that stabilization of the remaining austenite has occurred due to the bainitic transformation. However, it is also seen that the kinetics of martensite formation in all the partially bainitic samples can be well described using a constant value of the rate parameter $\alpha_m = 0.0131 \text{ K}^{-1}$. Figure 5 shows that the correlation between α_m and T_{KM} for partially bainitic samples Fe-0.80C (open triangles) is different from the trend between α_m and T_{KM} corresponding chemical stabilization (solid squares), as obtained for the intercritically annealed samples of Fe-0.46C and Fe0.66C discussed earlier. This indicates that the stabilization of the austenite due to the partial bainitic transformation is not of a chemical nature.

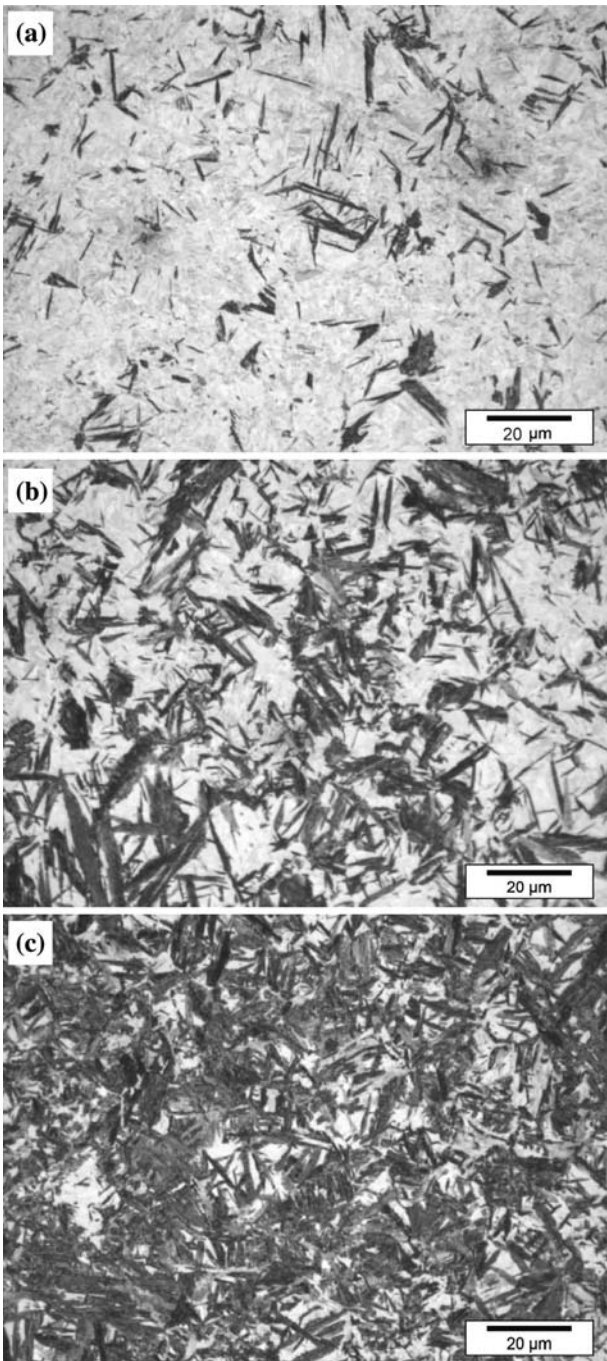


Fig. 7—Optical micrographs corresponding to the evolution of isothermal bainite formation in Fe-0.80C at 325 °C after (a) 2 min (15 vol pct), (b) 4 min (44 vol pct), and (c) 6 min (79 vol pct).

The conclusion drawn, *viz.* that the stabilization cannot be of a chemical nature, is strengthened by the following reasoning and analysis of the dilatometry results, which demonstrates that an explanation in terms of chemical stabilization is not self-consistent. If, contrary to the general opinion on lean-Si steels, carbon enrichment in austenite is assumed to occur in Fe-0.80-0.3Si during the partial transformation to bainite, the bainitic transformation after prolonged holding at which no length change is observed is considered to be

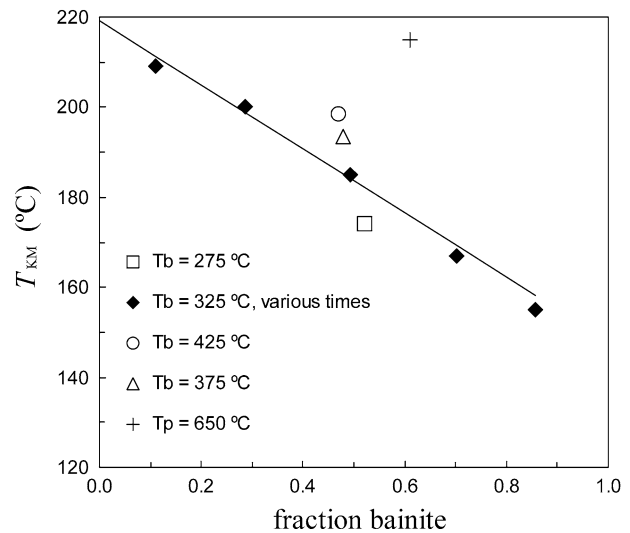


Fig. 8—Start-temperature T_{KM} of martensite formation in Fe-0.80C samples partially transformed to bainite at different temperatures and for different times at $T_b = 325$ °C. The solid line represents the linear dependence, which gives the best agreement with the observed decrease of T_{KM} with increasing fraction bainite at $T_b = 325$ °C (x_C^{γ} constant).

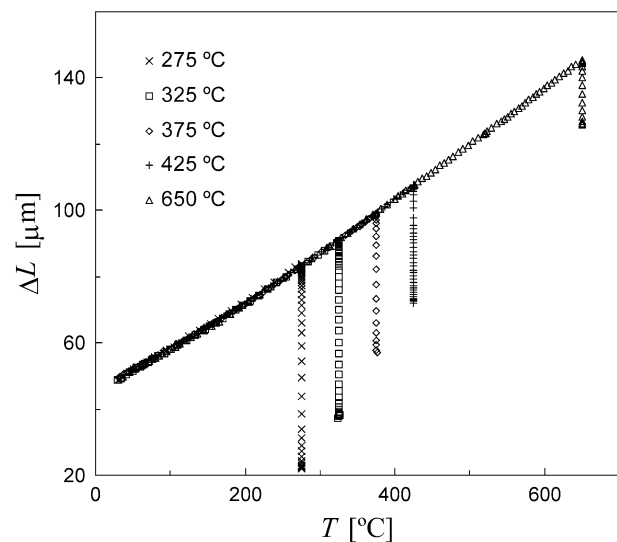


Fig. 9—Thermal contraction of Fe-0.80C samples, represented by the length change ΔL , as a function of temperature T after prolonged holding at various bainite formation temperatures. The thermal expansion is seen to be similar to a sample completely transformed to pearlite at 650 °C.

incomplete, the so-called “incomplete reaction phenomenon.”^[21] This implies a significant increasing fraction of remaining austenite with increasing bainitic holding temperature T_b , which affects the thermal expansion/contraction during cooling to room temperature. However, for the four different temperatures T_b in the range 275 °C to 425 °C, the thermal expansion is virtually identical, as shown in Figure 9. In fact, the thermal expansion is also the same as for a sample that was completely transformed to pearlite at $T = 650$ °C, and

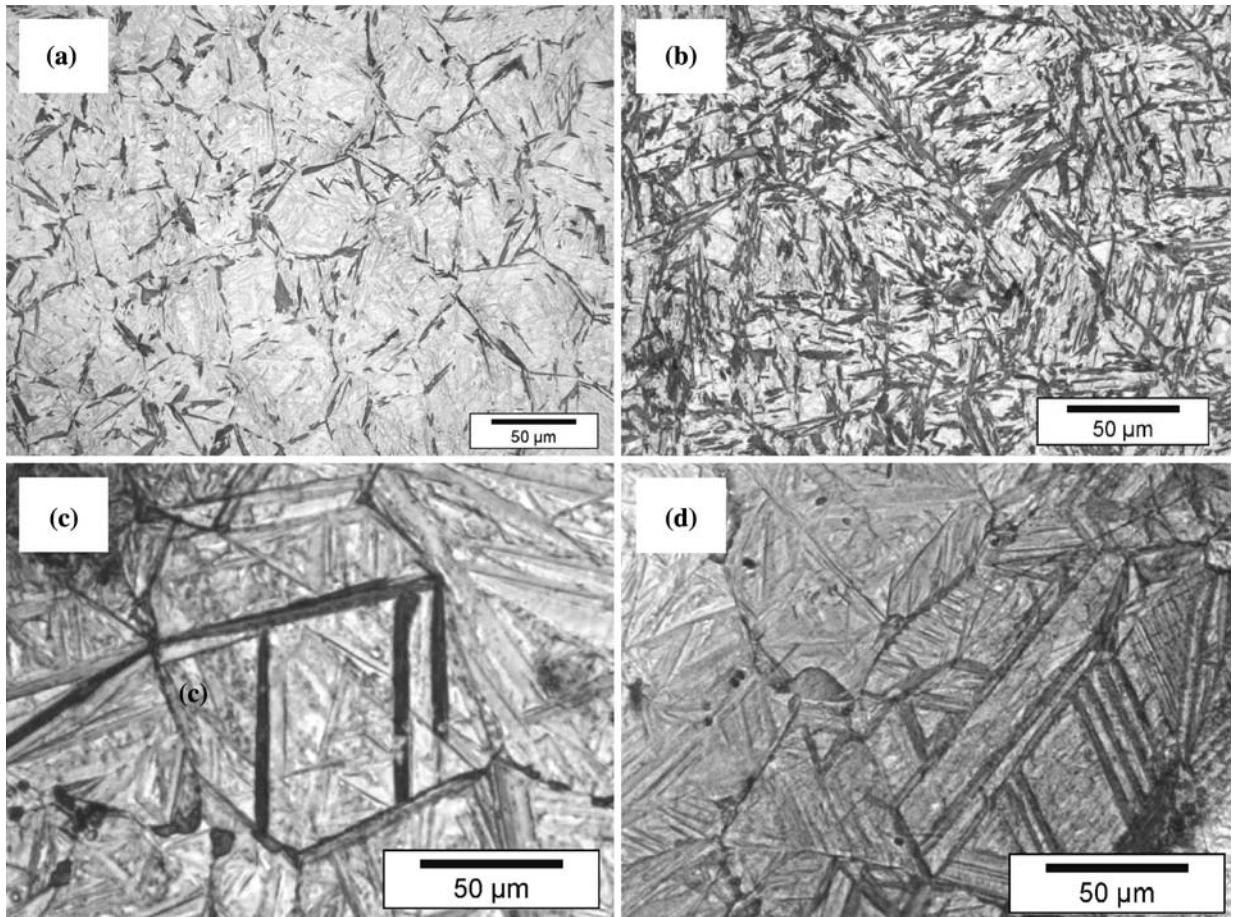


Fig. 10—(a) Microstructure after austenitizing at $T_{\text{aus}} = 1050$ °C, quenching to $T_1 = 210$ °C, tempering at $T_2 = 300$ °C, and cooling to room temperature. (b) Microstructure after austenitizing at $T_{\text{aus}} = 1050$ °C, quenching to $T_1 = 175$ °C, tempering at $T_2 = 300$ °C, and cooling to room temperature. (c) and (d) Microstructure at a polished surface after austenitizing at $T_{\text{aus}} = 1050$ °C, during which the austenite grain boundaries are revealed by thermal etching, and quenching to $T_1 = 245$ °C, tempering at $T_2 = 300$ °C, and cooling to room temperature.

subsequently cooled to room temperature. It can be calculated that a difference in the volume fraction austenite of more than 3 vol pct results in a significant difference in the thermal contraction, but this is clearly not observed in Figure 9.

D. Microstructural Analysis of the Evolution of Martensite Formation

To obtain a better understanding of the evolution of martensite in an austenitic matrix, the metallographic technique for measuring martensite first described by Greninger and Troiano^[1] was applied to various samples of Fe-0.80C. In this way, we can investigate where the martensite plates or laths are formed at the early stage of transformation and how the transformation evolves subsequently with decreasing temperature. The principles involved in this technique and the associated heat treatment have been described in detail by Grange and Stewart.^[2] They studied an eutectoid carbon steel and determined the kinetics of martensite formation by metallographic examination of samples that were first quenched to a certain temperature T_1 below M_s , and subsequently, the initially formed martensite was briefly

tempered at a temperature T_2 above M_s .^[2] After the tempering step, the samples were quenched to room temperature and etched with picral to distinguish the initial martensite, which is tempered, and thus dark etching, from the martensite formed during the final quench, which appears light gray. In the present study, a number of samples were heat treated according to the preceding procedure in order to identify the initially formed martensite in the final microstructure.

The microstructures of a sample Fe-0.80C with $T_{\text{aus}} = 1050$ °C, quenched to $T_1 = 210$ °C and tempered at $T_2 = 300$ °C, are shown in Figure 10(a). The dark-etched phase is the initially formed martensite. Figure 10(b) shows the microstructure at a later stage of transformation ($T_1 = 175$ °C), which indicates that the (40 to 50 pct) martensite formed is rather homogeneously distributed in the matrix. It is interesting to note that Grange and Stewart made very similar observations and that they suggested that the prior austenite grain boundaries are the most preferred regions for nucleation of martensite. Indeed, the dark-etching initially formed martensite in Figure 10(a) seems to outline the prior austenite grain structure at some regions, but the apparent grain size corresponding to the dark-etching

structure is rather small compared to the austenite grain size of approximately 130 μm . Therefore, additional experiments were conducted with the objective to reveal both the prior austenite grain structure and the first-formed martensite. Samples Fe-0.80C were polished prior to the Greninger–Troiano heat treatment. The microstructures observed at the polished surface after the heat treatment and picral etching are shown in Figures 10(c) and (d). It is seen that the first-formed martensite plates do not have a preference to form along the austenite grain boundary, but across austenite grains. Probably, the initially formed plates nucleate at a grain boundary and their growth is stopped at another grain boundary. It is noted that a free surface may alter the transformation behavior to some extent, because a free surface reduces the volumetric constraint around martensite plates. It is difficult to quantify this effect, but it may explain the markedly different martensite morphology seen in Figure 10(c) compared to Figure 10(a).

In relation to the preceding observations, it is noted that the hypothesis that the austenite grain boundaries are the preferred regions for nucleation of martensite cannot fully explain why M_s of a large-grained structure is higher^[8,10,11] and why the overall kinetics are virtually independent of the prior austenite grain size.^[7] On the contrary, one would expect that the overall kinetics would increase for a fine-grained structure if the grain boundaries are the preferred nucleation sites and nucleation is rate determining. However, this is not the case, and therefore, the γ grain boundaries cannot be envisaged to play a very important role at each stage of transformation. This is consistent with the work of Kajiwara, who also concluded that the nucleation of martensite is not simply related to grain boundaries, but that the plastic accommodation of the shape strain in austenite is the most important step in the event of martensite formation.^[8]

IV. DISCUSSION

A. Mechanical Stabilization of Austenite Due to a Displacive Transformation

Comparison of the evolution of martensite formation in samples Fe-0.80C with a bainitic/austenitic microstructure (Figure 6) with the transformation characteristics in Fe-0.46C and Fe0.66C with a ferritic/austenitic microstructure (Figures 3 and 4) indicates that the stabilization of the austenite during a partial bainitic transformation is of a different nature than the chemical stabilization of austenite during intercritical annealing. This difference in stabilization mechanism is also directly apparent from Figure 5, and based on these observations and considerations, it is argued that the linear decrease of T_{KM} with increasing fraction of bainite shown in Figure 8 (x_C^2 constant) is best explained by mechanical stabilization of the austenite.^[22,23] The displacive growth of bainite is accompanied with a shape change of the grains, which leads to a plastic deformation of the surrounding austenite. The increased strength of the austenite means that a higher driving force is needed to initiate the transformation to martensite, and therefore the start

temperature T_{KM} for the remaining austenite is decreased. It is also seen in Figure 8 that the stabilization effect becomes stronger at lower bainite formation temperatures. Probably, recovery of the plastically deformed austenite occurs concurrently with the transformation to bainite. The recovery is assumed to be more pronounced at high temperature, and therefore, the stabilization effect becomes less for higher T_b .

Based on the stabilizing effect of bainite, it seems plausible to assume that also the martensite strengthens the surrounding austenite during its formation, and that this mechanical stabilization impedes the plastic accommodation of the subsequent transformation. When a martensite lath or plate is formed, dislocations are generated in the surrounding austenite by plastic deformation due to the volumetric and shear strains. On the one hand, the dislocations produced in the austenite during transformation can assist the subsequent nucleation of martensite,^[24] which is known as autocatalytic nucleation.^[21] However, the dislocations induced in the austenite due to prior transformation can also retard the subsequent transformation to martensite, which is known as mechanical stabilization.^[22,23,25] The dislocation debris interferes with the movement of the glissile interface that constitutes the growth. When the strain buildup in the remaining austenite accompanying the transformation exceeds a critical value, the further transformation at a certain temperature below M_s is suppressed.^[26] In this sense, mechanical stabilization can play an essential role in the athermal character of the martensitic transformation in carbon steels.

B. Rationalization of the Athermal Transformation Kinetics

Consider that a decrease in temperature dT below M_s results in the formation of a new number of plates or laths per unit volume of austenite, dN , with an average volume V_m . The shape deformation accompanying the formation of this volume of martensite increases the strength of the remaining austenite and stops the transformation. The driving force at M_s is approximately 1700 J/mol, of which about 600 J/mol^[27,28] is considered to be stored in the surrounding austenite as strain energy E_S . Since the resistance of the remaining austenite against plastic deformation has increased due to the formation of dN plates, an increase in driving force is required for the transformation to recommence. It seems plausible to assume that the strain energy accompanying the subsequent transformation is larger, and that the increase in the required strain energy dE_S is proportional to the volume of martensite due to the temperature decrease dT and can be written as

$$dE_S = \chi V_m dN \quad [6]$$

with χ a proportionality constant. The change in volume fraction of martensite is given by^[6]

$$df = (1 - f) V_m dN \quad [7]$$

where $(1 - f)$ is the volume fraction of austenite available for further transformation. The transformation

progresses with decreasing temperature when dE_S is balanced by the increase of the chemical driving force of the remaining austenite $d(\Delta G)$:

$$dE_S = d(\Delta G) \quad [8]$$

By combining Eqs. [6] through Eq. [8], it follows that

$$df = (1 - f) \frac{1}{\chi} \frac{d(\Delta G)}{dT} dT \quad [9]$$

Solving this differential equation and integrating from T_{KM} ($f = 0$) to T leads to Eq. [1], the KM equation, with

$$\alpha_m = \frac{1}{\chi} \frac{d(\Delta G)}{dT} \quad [10]$$

Calculations with MT-DATA for Fe-0.80C yield a fairly constant value for $d(\Delta G)/dT = 6.9$ J/mol K, and analysis of the experimental kinetics of Fe-0.80C resulted in $\alpha_m = 0.0131$ K⁻¹. Using these values, it follows according to Eq. [10] that the proportionality constant $\chi = 523$ J/mol, which seems to be a reasonable value in view of the reported values of the stored strain energy.^[27,28] The values of χ for Fe-0.46C and Fe-0.66C are listed in Table IV and are of the same magnitude.

It is seen that χ increases with increasing carbon content, which is probably related to the result reported by Chatterjee and Bhadeshia that the critical value of the plastic strain becomes smaller as the carbon content of the austenite increases.^[27] The underlying reason for the fact that the rate parameter α_m becomes smaller with increasing carbon content (Eq. [2])^[14] is possibly related to a combination of both a relatively strong solid solution strengthening effect of carbon, which plays an important role in the resistance to the interface motion,^[27,29] and increased dislocation strengthening for higher carbon steels.

In the athermal martensite model proposed previously, it is assumed that the local austenite strength determines the transformation temperature of a certain region. The transformation of such a region to martensite leads to an increase in the strength of the surrounding austenite, and therefore, each austenite region has a specific decomposition temperature. Thus, in the present model, the nucleation at certain defects is not considered to be the rate-controlling step in the transformation, but the resistance of the austenitic parent phase to the growth of the nuclei. This explanation for the athermal nature of the martensitic transformation is consistent with the “growth-resistance of

austenite” hypothesis proposed by Edmondson and Ko.^[3] By means of metallographic examination, they demonstrated that the formation of martensite is accompanied by a reasonable amount of plastic deformation, and that the deformation has an effect on the subsequent transformation.

Based on the micrographs seen in Figure 10 and consideration of the local strength of the austenite that determines the resistance against plastic deformation and thus the strain energy involved in the formation of martensite plates or laths, it is postulated that the initial formation of martensite occurs preferably in the grain interior, which is assumed relatively soft compared to the grain boundary regions.^[11] The first-formed martensite plates effectively divide the prior austenite grain and strengthen the surrounding austenite, and the subsequent formation of martensite plates in the same grain require a larger driving force. This hypothesis is in accordance with the analysis by Kajiwara of the austenite yield stress and the driving force at M_s for Fe-Ni alloys.^[8] Kajiwara argued that the energy expended in deforming the austenite in order to accommodate the shear strain, W , is proportional to the yield stress, and he demonstrated that the increase in the required driving force for fine-grained specimens corresponds to an increase in W due to the increase in yield stress with grain refinement. This relationship proposed by Kajiwara is in general agreement with the starting assumptions of the KM relation in the present study, since it seems plausible to assume that the yield stress of the remaining austenite increases also due to the deformation induced by the displacive transformation itself.

V. CONCLUSIONS

The progress of martensite formation in partially and fully austenitic plain carbon steels has been determined using dilatometry. The characteristics of martensite formation in partially austenitic steels after intercritical annealing can be quantitatively explained by carbon enrichment of the remaining (intercritical) austenite. In contrast, this chemical stabilization mechanism of austenite cannot explain the transformation characteristics of the remaining austenite after a partial transformation to bainite in lean-Si steels. It is therefore concluded that the stabilization of austenite due to a partial transformation to bainite is of a mechanical nature: the austenite is strengthened due to the shape change accompanying the transformation. Finally, it is postulated that the typical progress of the transformation to martensite with decreasing temperature, which can be described by a natural decay function, the KM equation, is a consequence of the increase in strength of the remaining austenite as the transformation progresses. Thus, in the present model of the martensitic transformation, the plastic accommodation in the austenite of the deformation strain is considered to be the critical step in the formation of athermal martensite.

Table IV. The Rate Parameter α_m and the Proportionality Constant χ

Alloy	α_m (K ⁻¹)	$d(\Delta G)/dT$ (J/mol K)	χ (J/mol)
Fe-0.46C	0.0168	7.0	417
Fe-0.66C	0.0146	7.2	493
Fe-0.80C	0.0132	6.9	523

OPEN ACCESS

This article is distributed under the terms of the Creative Commons Attribution Noncommercial License which permits any noncommercial use, distribution, and reproduction in any medium, provided the original author(s) and source are credited.

REFERENCES

1. A.B. Greninger and A.R. Troiano: *Trans. ASM*, 1940, vol. 28, pp. 537–74.
2. R.A. Grange and H.M. Stewart: *Trans. AIME*, 1946, vol. 167, pp. 467–90.
3. B. Edmondson and T. Ko: *Acta Metall.*, 1954, vol. 2, pp. 235–41.
4. L. Kaufman and M. Cohen: *Prog. Met. Phys.*, 1958, vol. 7, pp. 165–246.
5. D.P. Koistinen and R.E. Marburger: *Acta Metall.*, 1959, vol. 7, pp. 59–60.
6. C.L. Magee: *Phase Transformations*, ASM, Metals Park, OH, 1970, pp. 115–55.
7. A.S. Sastri and D.R.F. West: *J. Iron Steel Inst.*, 1965, vol. 203, pp. 138–49.
8. S. Kajiwara: *Metall. Trans. A*, 1986, vol. 17A, pp. 1693–702.
9. E.M. Breinan and G.S. Ansell: *Metall. Trans.*, 1970, vol. 1, pp. 1513–23.
10. T.J. Nichol, G. Judd, and G.S. Ansell: *Metall. Trans. A*, 1977, vol. 8A, pp. 1877–83.
11. P.J. Brofman and G.S. Ansell: *Metall. Trans. A*, 1983, vol. 14A, pp. 1929–31.
12. T.A. Kop, J. Sietsma, and S. Van der Zwaag: *J. Mater. Sci.*, 2001, vol. 36, pp. 519–26.
13. S.M.C. Van Bohemen, M.J. Santofimia, and J. Sietsma: *Scripta Mater.*, 2008, vol. 58, pp. 488–91.
14. S.M.C. Van Bohemen and J. Sietsma: *Mater. Sci. Technol.*, in press, DOI [10.1179/174328408X365838](https://doi.org/10.1179/174328408X365838).
15. E. Gillam and D.G. Cole: *Phil. Mag.*, 1953, vol. 44, pp. 999–1009.
16. R. Pradhan and G.S. Ansell: *Metall. Trans. A*, 1978, vol. 9A, pp. 793–801.
17. K.W. Andrews: *J. Iron Steel Inst.*, 1965, vol. 203, pp. 721–29.
18. P. Payson and C.H. Savage: *Trans. ASM*, 1944, vol. 33, pp. 261–75.
19. A.E. Nehrenberg: *Trans. AIME*, 1946, vol. 167, pp. 494–98.
20. P.J. Jacques, E. Girault, P. Harlet, and F. Delannay: *ISIJ Int.*, 2001, vol. 41, pp. 1061–70.
21. H.K.D.H. Bhadeshia: *Bainite in Steels*, The Institute of Materials, London, 2001.
22. E.S. Machlin and M. Cohen: *Trans. AIME*, 1951, vol. 191, pp. 267–74.
23. J.R. Strife, M.J. Carr, and G.S. Ansell: *Metall. Trans. A*, 1977, vol. 8A, pp. 1471–83.
24. G.B. Olson and M. Cohen: *Metall. Trans. A*, 1975, vol. 6A, pp. 791–95.
25. H.K.D.H. Bhadeshia: *Mater. Sci. Eng. A*, 1999, vol. 275, pp. 58–66.
26. S. Chatterjee, H.S. Wang, J.R. Yang, and H. Bhadeshia: *Mater. Sci. Technol.*, 2006, vol. 22, pp. 641–44.
27. S. Chatterjee and H.K.D.H. Bhadeshia: *Mater. Sci. Technol.*, 2007, vol. 23, pp. 1101–04.
28. J.W. Christian: in *ICOMAT '79*, G.B. Olson and M. Cohen, eds., MIT, Boston, MA, 1979, pp. 145–54.
29. K.J. Irvine, T. Gladman, and F.B. Pickering: *J. Iron Steel Inst.*, 1969, vol. 207, pp. 1017–28.